
9.1. Clutter Definition

Clutter is a term used to describe any object that may generate unwanted radar returns that may interfere with normal radar operations. Parasitic returns that enter the radar through the antenna's main lobe are called main lobe clutter; otherwise they are called side lobe clutter. Clutter can be classified in two main categories: surface clutter and airborne or volume clutter. Surface clutter includes trees, vegetation, ground terrain, man-made structures, and sea surface (sea clutter). Volume clutter normally has large extent (size) and includes chaff, rain, birds, and insects. Chaff consists of a large number of small dipole reflectors that have large RCS values. It is released by hostile aircraft or missiles as a means of ECM in an attempt to confuse the defense. Surface clutter changes from one area to another, while volume clutter may be more predictable.

Clutter echoes are random and have thermal noise-like characteristics because the individual clutter components (scatterers) have random phases and amplitudes. In many cases, the clutter signal level is much higher than the receiver noise level. Thus, the radar's ability to detect targets embedded in high clutter background depends on the Signal-to-Clutter Ratio (SCR) rather than the SNR.

White noise normally introduces the same amount of noise power across all radar range bins, while clutter power may vary within a single range bin. And since clutter returns are target-like echoes, the only way a radar can distinguish target returns from clutter echoes is based on the target RCS σ_t , and the anticipated clutter RCS σ_c (via clutter map). Clutter RCS can be defined as the equivalent radar cross section attributed to reflections from a clutter area, A_c . The average clutter RCS is given by

$$\sigma_c = \sigma^0 A_c \quad (9.1)$$

where $\sigma^0 (m^2/m^2)$ is the clutter scattering coefficient, a dimensionless quantity that is often expressed in dB. Some radar engineers express σ^0 in terms of squared centimeters per squared meter. In these cases, σ^0 is 40dB higher than normal.

The term that describes the constructive/destructive interference of the electromagnetic waves diffracted from an object (target or clutter) is called the propagation factor (see Chapter 8 for more details). Since target and clutter returns have different angles of arrival (different propagation factors), we can define the SCR as

$$SCR = \frac{\sigma_t F_t^2 F_r^2}{\sigma_c F_c^2} \quad (9.2)$$

where F_c is the clutter propagation factor, F_t and F_r are, respectively, the transmit and receive propagation factors for the target. In many cases $F_t = F_r$.

9.2. Surface Clutter

Surface clutter includes both land and sea clutter, and is often called area clutter. Area clutter manifests itself in airborne radars in the look-down mode. It is also a major concern for ground-based radars when searching for targets at low grazing angles. The grazing angle ψ_g is the angle from the surface of the earth to the main axis of the illuminating beam, as illustrated in Fig. 9.1.

Three factors affect the amount of clutter in the radar beam. They are the grazing angle, surface roughness, and the radar wavelength. Typically, the clutter scattering coefficient σ^0 is larger for smaller wavelengths. Fig. 9.2 shows a sketch describing the dependency of σ^0 on the grazing angle. Three regions are identified; they are the low grazing angle region, flat or plateau region, and the high grazing angle region.

The low grazing angle region extends from zero to about the critical angle. The critical angle is defined by Rayleigh as the angle below which a surface is considered to be smooth, and above which a surface is considered to be rough. Denote the root mean square (rms) of a surface height irregularity as h_{rms} , then according to the Rayleigh criteria the surface is considered to be smooth if

$$\frac{4\pi h_{rms}}{\lambda} \sin \psi_g < \frac{\pi}{2} \quad (9.3)$$

Consider a wave incident on a rough surface, as shown in Fig. 9.3. Due to surface height irregularity (surface roughness), the “rough path” is longer than the “smooth path” by a distance $2h_{rms} \sin \psi_g$. This path difference translates into a phase differential $\Delta\psi$:

$$\Delta\psi = \frac{2\pi}{\lambda} 2h_{rms} \sin \psi_g \quad (9.4)$$

The critical angle ψ_{gc} is then computed when $\Delta\psi = \pi$ (first null), thus

$$\frac{4\pi h_{rms}}{\lambda} \sin \psi_{gc} = \pi \quad (9.5)$$

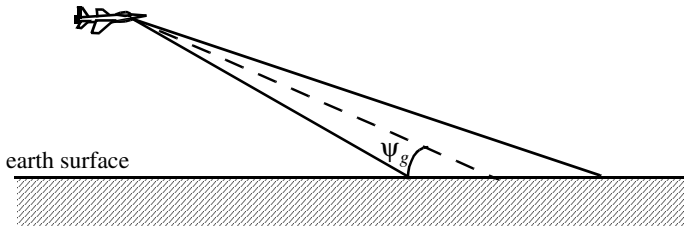


Figure 9.1. Definition of grazing angle.

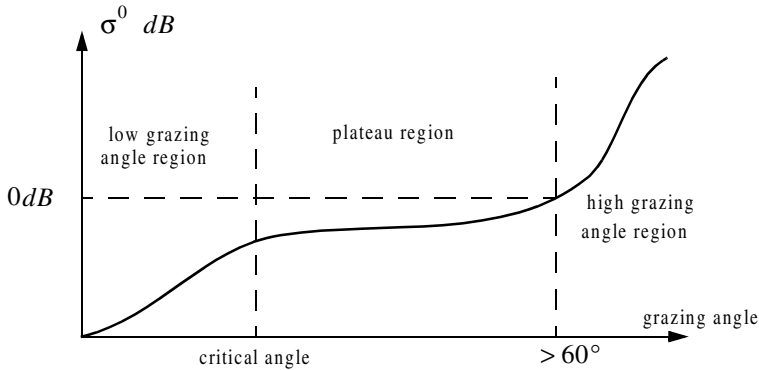


Figure 9.2. Clutter regions.

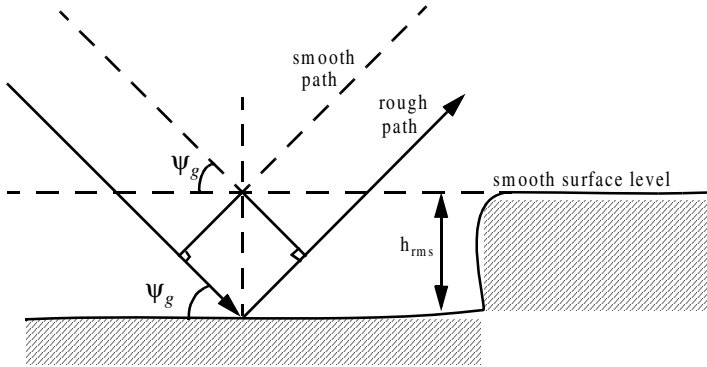


Figure 9.3. Rough surface definition.

or equivalently,

$$\Psi_{gc} = \text{asin} \frac{\lambda}{4h_{rms}} \quad (9.6)$$

In the case of sea clutter, for example, the rms surface height irregularity is

$$h_{rms} \approx 0.025 + 0.046 S_{state}^{1.72} \quad (9.7)$$

where S_{state} is the sea state, which is tabulated in several cited references. The sea state is characterized by the wave height, period, length, particle velocity, and wind velocity. For example, $S_{state} = 3$ refers to a moderate sea state, where in this case the wave height is approximately equal to between 0.9144 to 1.2192 m, the wave period 3.5 to 4.5 seconds, wave length 1.9812 to 33.528 m, wave velocity 20.372 to 25.928 Km/hr, and wind velocity 22.224 to 29.632 Km/hr.

Clutter at low grazing angles is often referred to as diffused clutter, where there are a large number of clutter returns in the radar beam (non-coherent reflections). In the flat region the dependency of σ^0 on the grazing angle is minimal. Clutter in the high grazing angle region is more specular (coherent reflections) and the diffuse clutter components disappear. In this region the smooth surfaces have larger σ^0 than rough surfaces, opposite of the low grazing angle region.

9.2.1. Radar Equation for Area Clutter

Consider an airborne radar in the look-down mode shown in Fig. 9.4. The intersection of the antenna beam with ground defines an elliptically shaped footprint. The size of the footprint is a function of the grazing angle and the antenna 3dB beam width θ_{3dB} , as illustrated in Fig. 9.5. The footprint is divided into many ground range bins each of size $(c\tau/2)\sec\psi_g$, where τ is the pulse width.

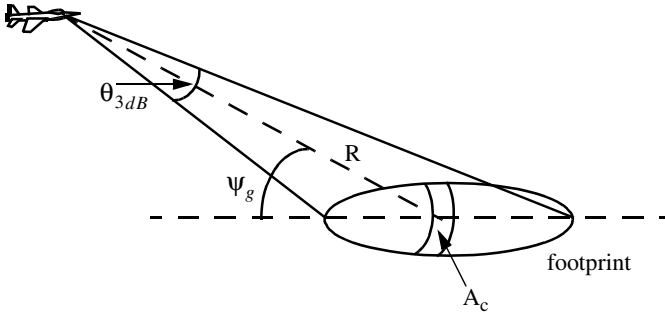


Figure 9.4. Airborne radar in the look-down mode.

From Fig. 9.5, the clutter area A_c is

$$A_c \approx R\theta_{3dB}\frac{c\tau}{2}\sec\psi_g \quad (9.8)$$

The power received by the radar from a scatterer within A_c is given by the radar equation as

$$S_t = \frac{P_t G^2 \lambda^2 \sigma_t}{(4\pi)^3 R^4} \quad (9.9)$$

where as usual, P_t is the peak transmitted power, G is the antenna gain, λ is the wavelength, and σ_t is the target RCS. Similarly, the received power from clutter is

$$S_{A_c} = \frac{P_t G^2 \lambda^2 \sigma_c}{(4\pi)^3 R^4} \quad (9.10)$$

where the subscript A_c is used for area clutter. Substituting Eq. (9.1) for σ_c into Eq. (9.10), we can then obtain the SCR for area clutter by dividing Eq. (9.9) by Eq. (9.10). More precisely,

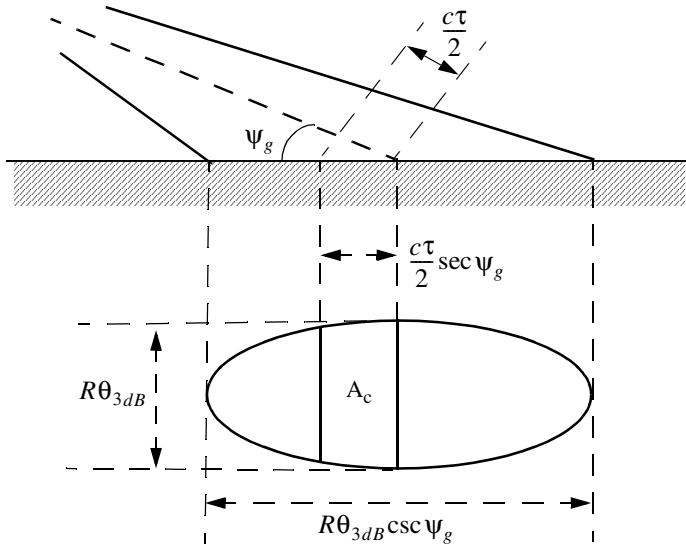


Figure 9.5. Footprint definition.

$$(SCR)_{Ac} = \frac{2\sigma_t \cos \psi_g}{\sigma^0 \theta_{3dB} R c \tau} \quad (9.11)$$

Example 9.1: Consider an airborne radar shown in Fig. 9.4. Let the antenna 3dB beam width be $\theta_{3dB} = 0.02 \text{ rad}$, the pulse width $\tau = 2 \mu\text{s}$, range $R = 20 \text{ Km}$, and grazing angle $\psi_g = 20^\circ$. Assume target RCS $\sigma_t = 1 \text{ m}^2$, and clutter reflection coefficient $\sigma^0 = 0.0136 \text{ m}^2/\text{m}^2$. Compute the SCR.

Solution: The SCR is given by Eq. (9.11) as

$$(SCR)_{Ac} = \frac{2\sigma_t \cos \psi_g}{\sigma^0 \theta_{3dB} R c \tau} \Rightarrow$$

$$(SCR)_{Ac} = \frac{(2)(1)(\cos 20)}{(0.0136)(0.02)(20000)(3 \times 10^8)(2 \times 10^{-6})} = 2.48 \times 10^{-4}$$

It follows that

$$(SCR)_{Ac} = -36.06 \text{ dB}$$

Thus, for reliable detection the radar must somehow increase its SCR by at least $(36 + X) \text{ dB}$, where X is on the order of 10 dB or better.

9.3. Volume Clutter

Volume clutter has large extents and includes rain (weather), chaff, birds, and insects. The volume clutter coefficient is normally expressed in squared meters (RCS per resolution volume). Birds, insects, and other flying particles are often referred to as angel clutter or biological clutter. The average RCS for individual birds or insects as a function of the weight of the bird or insect is reported in the literature¹ as

$$(\sigma_b)_{dBsm} \approx -46 + 5.8 \log W_b \quad (9.12)$$

where W_b is the individual bird or insect weight in grams. Bird and insect RCSs are also a function of frequency; for example, a pigeon's average RCS is $-26dBsm$ at S-band, and is equal to $-27dBsm$ at X-band.

As mentioned earlier, chaff is used as an ECM technique by hostile forces. It consists of a large number of dipole reflectors with large RCS values. Historically, chaff was made of aluminum foil; however, in recent years most chaff is made of the more rigid fiber glass with conductive coating. The maximum chaff RCS occurs when the dipole length L is one half the radar wavelength. The average RCS for a single dipole when viewed broadside is

$$\sigma_{chaff1} \approx 0.88\lambda^2 \quad (9.13)$$

and for an average aspect angle, it drops to

$$\sigma_{chaff1} \approx 0.15\lambda^2 \quad (9.14)$$

where the subscript *chaff1* is used to indicate a single dipole, and λ is the radar wavelength. The total chaff RCS within a radar resolution volume is

$$\sigma_{chaff} \approx 0.15\lambda^2 N_D \quad (9.15)$$

where N_D is the total number of dipoles in the resolution volume.

Weather or rain clutter is easier to suppress than chaff, since rain droplets can be viewed as perfect small spheres. We can use the Rayleigh approximation of perfect sphere to estimate the rain droplets' RCS. The Rayleigh approximation, without regard to the propagation medium index of refraction, is given in Eq. (2.30) and is repeated here as Eq. (9.16):

$$\sigma = 9\pi r^2 (kr)^4 \quad r \ll \lambda \quad (9.16)$$

where $k = 2\pi/\lambda$, and r is radius of a rain droplet.

1. Edde, B., *Radar - Principles, Technology, Applications*, Prentice-Hall, 1993.

Electromagnetic waves when reflected from a perfect sphere become strongly co-polarized (have the same polarization as the incident waves). Consequently, if the radar transmits, say, a right-hand-circularly (RHC) polarized wave, then the received waves are left-hand-circularly (LHC) polarized, because it is propagating in the opposite direction. Therefore, the back-scattered energy from rain droplets retains the same wave rotation (polarization) as the incident wave, but has a reversed direction of propagation. It follows that radars can suppress rain clutter by co-polarizing the radar transmit and receive antennas.

Defining η as RCS per unit resolution volume V_W , it is computed as the sum of all individual scatterers RCS within the volume,

$$\eta = \sum_{i=1}^N \sigma_i \quad (9.17)$$

where N is the total number of scatterers within the resolution volume. Thus, the total RCS of a single resolution volume is

$$\sigma_W = \sum_{i=1}^N \sigma_i V_W \quad (9.18)$$

A resolution volume is shown in Fig. 9.6, and is approximated by

$$V_W \approx \frac{\pi}{8} \theta_a \theta_e R^2 c \tau \quad (9.19)$$

where θ_a , θ_e are, respectively, the antenna beam width in azimuth and elevation, τ is the pulse width in seconds, c is speed of light, and R is range.

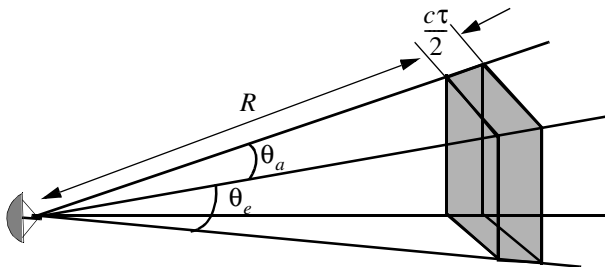


Figure 9.6. Definition of a resolution volume.

Consider a propagation medium with an index of refraction m . The i th rain droplet RCS approximation in this medium is

$$\sigma_i \approx \frac{\pi^5}{\lambda^4} K^2 D_i^6 \quad (9.20)$$

where

$$K^2 = \left| \frac{m^2 - 1}{m^2 + 2} \right|^2 \quad (9.21)$$

and D_i is the i th droplet diameter. For example, temperatures between $32^\circ F$ and $68^\circ F$ yield

$$\sigma_i \approx 0.93 \frac{\pi^5}{\lambda^4} D_i^6 \quad (9.22)$$

and for ice Eq. (9.20) can be approximated by

$$\sigma_i \approx 0.2 \frac{\pi^5}{\lambda^4} D_i^6 \quad (9.23)$$

Substituting Eq. (9.20) into Eq. (9.17) yields

$$\eta = \frac{\pi^5}{\lambda^4} K^2 Z \quad (9.24)$$

where the weather clutter coefficient Z is defined as

$$Z = \sum_{i=1}^N D_i^6 \quad (9.25)$$

In general, a rain droplet diameter is given in millimeters and the radar resolution volume is expressed in cubic meters, thus the units of Z are often expressed in *millimeter*⁶/*m*³.

9.3.1. Radar Equation for Volume Clutter

The radar equation gives the total power received by the radar from a σ_t target at range R as

$$S_t = \frac{P_t G^2 \lambda^2 \sigma_t}{(4\pi)^3 R^4} \quad (9.26)$$

where all parameters in Eq. (9.26) have been defined earlier. The weather clutter power received by the radar is

$$S_W = \frac{P_t G^2 \lambda^2 \sigma_W}{(4\pi)^3 R^4} \quad (9.27)$$

Using Eq. (9.18) and Eq. (9.19) into Eq. (9.27) and collecting terms yield

$$S_W = \frac{P_t G^2 \lambda^2}{(4\pi)^3 R^4} \frac{\pi}{8} R^2 \theta_a \theta_e c \tau \sum_{i=1}^N \sigma_i \quad (9.28)$$

The SCR for weather clutter is then computed by dividing Eq. (9.26) by Eq. (9.28). More precisely,

$$(SCR)_V = \frac{S_t}{S_W} = \frac{8\sigma_t}{\pi \theta_a \theta_e c \tau R^2 \sum_{i=1}^N \sigma_i} \quad (9.29)$$

where the subscript V is used to denote volume clutter.

Example 9.2: A certain radar has target RCS $\sigma_t = 0.1m^2$, pulse width $\tau = 0.2\mu s$, antenna beam width $\theta_a = \theta_e = 0.02radians$. Assume the detection range to be $R = 50Km$, and compute the SCR if $\sum \sigma_i = 1.6 \times 10^{-8}(m^2/m^3)$.

Solution: From Eq. (9.29) we have

$$(SCR)_V = \frac{8\sigma_t}{\pi \theta_a \theta_e c \tau R^2 \sum_{i=1}^N \sigma_i}$$

substituting the proper values we get

$$(SCR)_V = \frac{(8)(0.1)}{\pi(0.02)^2(3 \times 10^8)(0.2 \times 10^{-6})(50 \times 10^3)^2(1.6 \times 10^{-8})} = 0.265$$

$$(SCR)_V = -5.768dB.$$

9.4. Clutter Statistical Models

Since clutter within a resolution cell (or volume) is composed of a large number of scatterers with random phases and amplitudes, it is statistically described by a probability distribution function. The type of distribution depends on the nature of clutter itself (sea, land, volume), the radar operating frequency, and the grazing angle.

If sea or land clutter is composed of many small scatterers when the probability of receiving an echo from one scatterer is statistically independent of the echo received from another scatterer, then the clutter may be modeled using a Rayleigh distribution,

$$f(x) = \frac{2x}{x_0} \exp\left(-\frac{x^2}{x_0}\right) ; x \geq 0 \quad (9.30)$$

where x_0 is the mean squared value of x .

The log-normal distribution best describes land clutter at low grazing angles. It also fits sea clutter in the plateau region. It is given by

$$f(x) = \frac{1}{\sigma\sqrt{2\pi} x} \exp\left(-\frac{(\ln x - \ln x_m)^2}{2\sigma^2}\right) ; x > 0 \quad (9.31)$$

where x_m is the median of the random variable x , and σ is the standard deviation of the random variable $\ln(x)$.

The Weibull distribution is used to model clutter at low grazing angles (less than five degrees) for frequencies between 1 and 10GHz. The Weibull probability density function is determined by the Weibull slope parameter a (often tabulated) and a median scatter coefficient $\bar{\sigma}_0$, and is given by

$$f(x) = \frac{bx^{b-1}}{\bar{\sigma}_0} \exp\left(-\frac{x^b}{\bar{\sigma}_0}\right) ; x \geq 0 \quad (9.32)$$

where $b = 1/a$ is known as the shape parameter. Note that when $b = 2$ the Weibull distribution becomes a Rayleigh distribution.

9.5. Clutter Spectrum

The power spectrum of stationary clutter (zero Doppler) can be represented by a delta function. However, clutter is not always stationary; it actually exhibits some Doppler frequency spread because of wind speed and motion of the radar scanning antenna. In general, the clutter spectrum is concentrated around

$f = 0$ and integer multiples of the radar PRF f_r , and may exhibit some small spreading.

The clutter power spectrum can be written as the sum of fixed (stationary) and random (due to frequency spreading) components. For most cases, the random component is Gaussian. If we denote the fixed to the random power ratio by W^2 , then we can write the clutter spectrum as

$$S_c(\omega) = \bar{\sigma}_0 \left(\frac{W^2}{1 + W^2} \right) \delta(\omega_0) + \frac{\bar{\sigma}_0}{(1 + W^2) \sqrt{2\pi\sigma_\omega^2}} \exp\left(-\frac{(\omega - \omega_0)^2}{2\sigma_\omega^2} \right) \quad (9.33)$$

where $\omega_0 = 2\pi f_0$ is the radar operating frequency in radians per second, σ_ω is the rms frequency spread component (determines the Doppler frequency spread), and $\bar{\sigma}_0$ is the Weibull parameter.

The first term of the right-hand side of Eq. (9.33) represents the PSD for stationary clutter, while the second term accounts for the frequency spreading. Nevertheless, since most of the clutter power is concentrated around zero Doppler with some spreading (typically less than 100 Hz), it is customary to model clutter using a Gaussian-shaped power spectrum (which is easier to analyze than Eq. (9.33)). More precisely,

$$S_c(\omega) = \frac{P_c}{\sqrt{2\pi\sigma_\omega^2}} \exp\left(-\frac{(\omega - \omega_0)^2}{2\sigma_\omega^2} \right) \quad (9.34)$$

where P_c is the total clutter power; σ_ω^2 and ω_0 were defined earlier. Fig. 9.7 shows a typical PSD sketch of radar returns when both target and clutter are present. Note that the clutter power is concentrated around DC and integer multiples of the PRF.

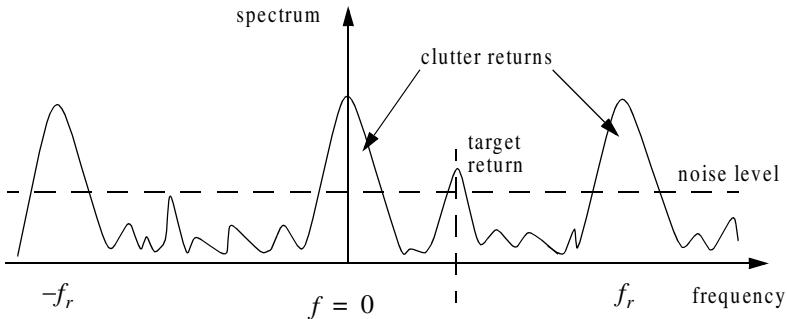


Figure 9.7. Typical radar return PSD when clutter and target are present.

9.6. Moving Target Indicator (MTI)

Clutter spectrum is normally concentrated around DC ($f = 0$) and multiple integers of the radar PRF f_r , as illustrated in Fig. 9.8a. In CW radars, clutter is avoided or suppressed by ignoring the receiver output around DC, since most of the clutter power is concentrated about the zero frequency band. Pulsed radar systems may utilize special filters that can distinguish between slowly moving or stationary targets and fast moving ones. This class of filters is known as the Moving Target Indicator (MTI). In simple words, the purpose of an MTI filter is to suppress target-like returns produced by clutter, and allow returns from moving targets to pass through with little or no degradation. In order to effectively suppress clutter returns, an MTI filter needs to have a deep stop-band at DC and at integer multiples of the PRF. Fig. 9.8b shows a typical sketch of an MTI filter response, while Fig. 9.8c shows its output when the PSD shown in Fig. 9.8a is the input.

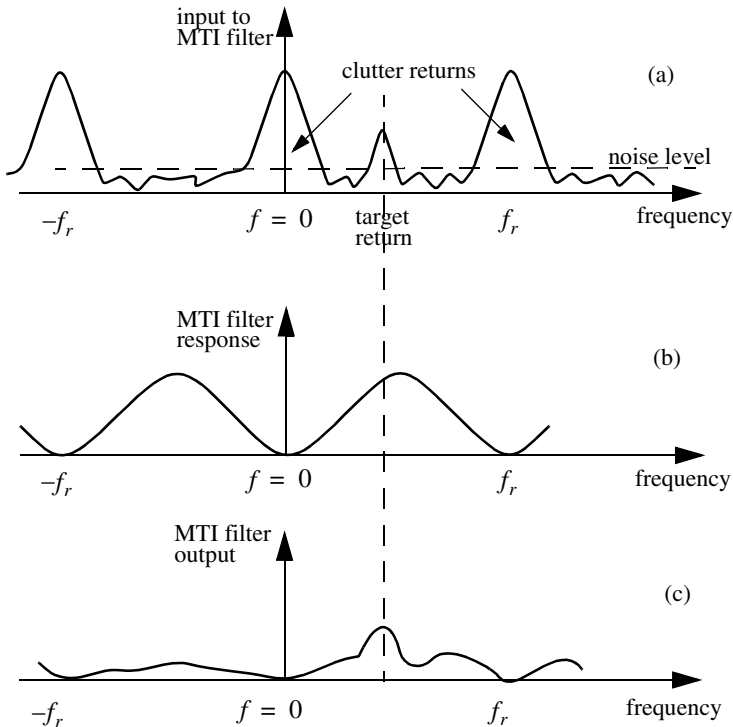


Figure 9.8. (a) Typical radar return PSD when clutter and target are present. (b) MTI filter frequency response. (c) Output from an MTI filter.

MTI filters can be implemented using delay line cancelers. As we will show later in this chapter, the frequency response of this class of MTI filters is periodic, with nulls at integer multiples of the PRF. Thus, targets with Doppler frequencies equal to nf_r are severely attenuated. And since Doppler is proportional to target velocity ($f_d = 2v/\lambda$), target speeds that produce Doppler frequencies equal to integer multiples of f_r are known as blind speeds. More precisely,

$$v_{blind} = \frac{\lambda f_r}{2} ; n \geq 0 \tag{9.35}$$

Radar systems can minimize the occurrence of blind speeds by either employing multiple PRF schemes (PRF staggering) or by using high PRFs where in this case the radar may become range ambiguous. The main difference between PRF staggering and PRF agility is that the pulse repetition interval (within an integration interval) can be changed between consecutive pulses for the case of PRF staggering.

Fig. 9.9 shows a block diagram of a coherent MTI radar. Coherent transmission is controlled by the STABLE Local Oscillator (STALO). The outputs of the STALO, f_{LO} , and the COHERENT Oscillator (COHO), f_C , are mixed to produce the transmission frequency, $f_{LO} + f_C$. The Intermediate Frequency (IF), $f_C \pm f_d$, is produced by mixing the received signal with f_{LO} . After the IF amplifier, the signal is passed through a phase detector and is converted into a base band. Finally, the video signal is inputted into an MTI filter.

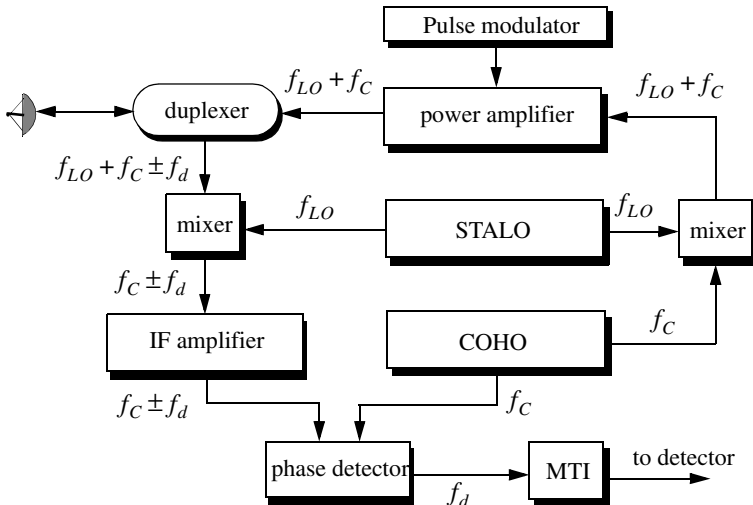


Figure 9.9. Coherent MTI radar block diagram.

9.7. Single Delay Line Canceler

A single delay line canceler can be implemented as shown in Fig. 9.10. The canceler's impulse response is denoted as $h(t)$. The output $y(t)$ is equal to the convolution between the impulse response $h(t)$ and the input $x(t)$. The single delay canceler is often called a "two-pulse canceler" since it requires two distinct input pulses before an output can be read.

The delay T is equal to the PRI of the radar ($1/f_r$). The output signal $y(t)$ is

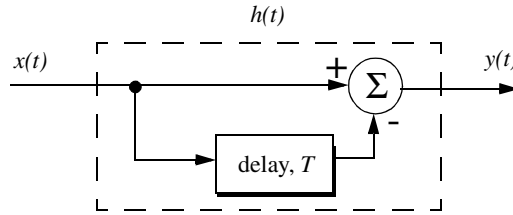


Figure 9.10. Single delay line canceler.

$$y(t) = x(t) - x(t - T) \quad (9.36)$$

The impulse response of the canceler is given by

$$h(t) = \delta(t) - \delta(t - T) \quad (9.37)$$

where $\delta(\cdot)$ is the delta function. It follows that the Fourier transform (FT) of $h(t)$ is

$$H(\omega) = 1 - e^{-j\omega T} \quad (9.38)$$

where $\omega = 2\pi f$.

In the z-domain, the single delay line canceler response is

$$H(z) = 1 - z^{-1} \quad (9.39)$$

The power gain for the single delay line canceler is given by

$$|H(\omega)|^2 = H(\omega)H^*(\omega) = (1 - e^{-j\omega T})(1 - e^{j\omega T}) \quad (9.40)$$

It follows that

$$|H(\omega)|^2 = 1 + 1 - (e^{j\omega T} + e^{-j\omega T}) = 2(1 - \cos \omega T) \quad (9.41)$$

and using the trigonometric identity $(2 - 2\cos 2\vartheta) = 4(\sin \vartheta)^2$ yields

$$|H(\omega)|^2 = 4(\sin(\omega T/2))^2 \quad (9.42)$$

MATLAB Function “single_canceler.m”

The function “single_canceler.m” computes and plots (as a function of f/f_r) the amplitude response for a single delay line canceler. It is given in Listing 9.1 in Section 9.14. The syntax is as follows:

$$[resp] = single_canceler(fofr)$$

where $fofr$ is the number of periods desired. Typical output of the function “single_canceler.m” is shown in Fig. 9.11. Clearly, the frequency response of a single canceler is periodic with a period equal to f_r . The peaks occur at $f = (2n + 1)/(2f_r)$, and the nulls are at $f = nf_r$, where $n \geq 0$.

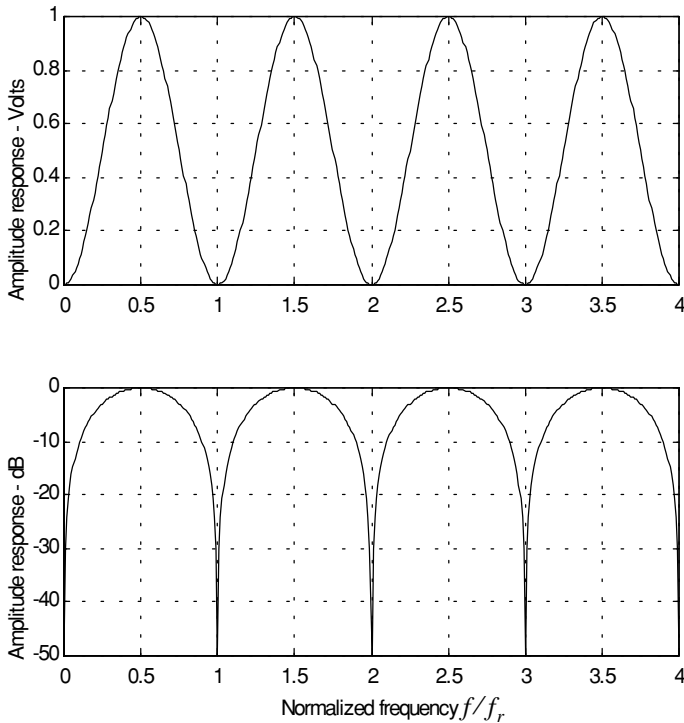


Figure 9.11. Single canceler frequency response.

In most radar applications the response of a single canceler is not acceptable since it does not have a wide notch in the stop-band. A double delay line canceler has better response in both the stop- and pass-bands, and thus it is more frequently used than a single canceler. In this book, we will use the names “single delay line canceler” and “single canceler” interchangeably.

9.8. Double Delay Line Canceler

Two basic configurations of a double delay line canceler are shown in Fig. 9.12. Double cancelers are often called “three-pulse cancelers” since they require three distinct input pulses before an output can be read. The double line canceler impulse response is given by

$$h(t) = \delta(t) - 2\delta(t - T) + \delta(t - 2T) \tag{9.43}$$

Again, the names “double delay line” canceler and “double canceler” will be used interchangeably. The power gain for the double delay line canceler is

$$|H(\omega)|^2 = |H_1(\omega)|^2 |H_1(\omega)|^2 \tag{9.44}$$

where $|H_1(\omega)|^2$ is the single line canceler power gain given in Eq. (9.42). It follows that

$$|H(\omega)|^2 = 16 \left(\sin\left(\frac{\omega T}{2}\right) \right)^4 \tag{9.45}$$

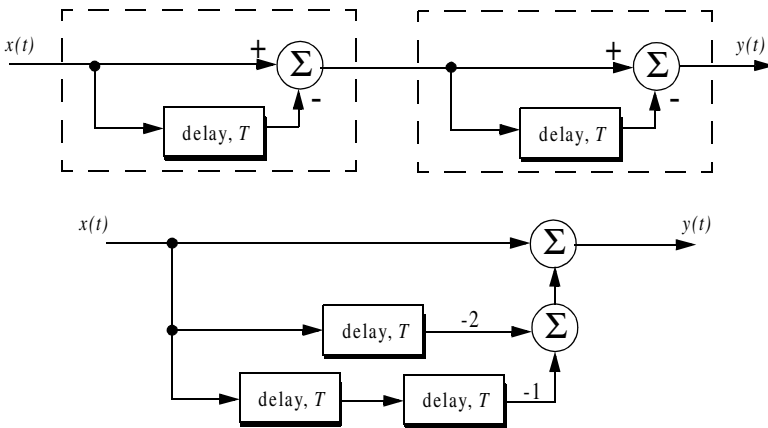


Figure 9.12. Two configurations for a double delay line canceler.

And in the z-domain, we have

$$H(z) = (1 - z^{-1})^2 = 1 - 2z^{-1} + z^{-2} \tag{9.46}$$

MATLAB Function “double_canceler.m”

The function “single_canceler.m” computes and plots (as a function of f/f_r) the amplitude response for a single delay line canceler. It is given in Listing 9.2 in Section 9.14. The syntax is as follows:

$$[resp] = double_canceler(fofr)$$

where $fofr$ is the number of periods desired.

Fig. 9.13 shows typical output from this function. Note that the double canceler has a better response than the single canceler (deeper notch and flatter pass-band response).

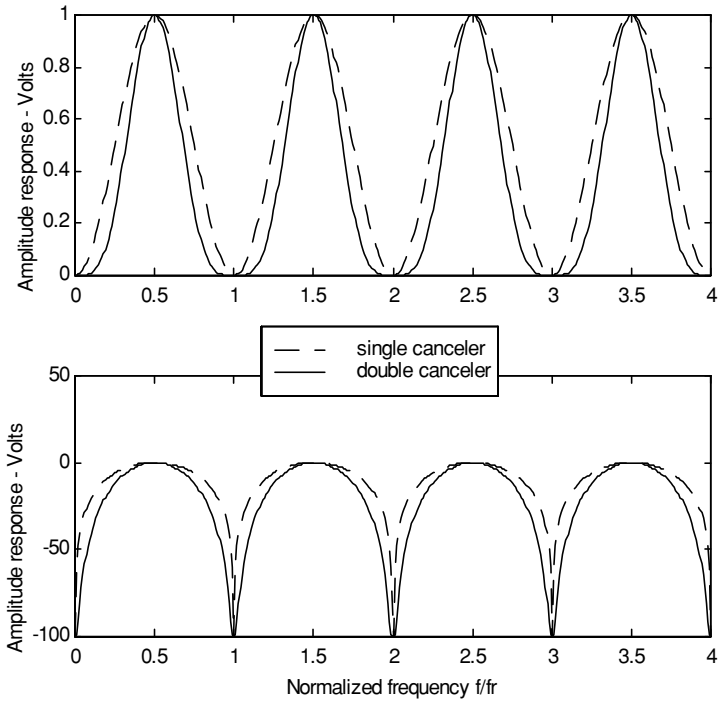


Figure 9.13. Normalized frequency responses for single and double cancelers.

9.9. Delay Lines with Feedback (Recursive Filters)

Delay line cancelers with feedback loops are known as recursive filters. The advantage of a recursive filter is that through a feedback loop we will be able to shape the frequency response of the filter. As an example, consider the single canceler shown in Fig. 9.14. From the figure we can write

$$y(t) = x(t) - (1 - K)w(t) \quad (9.47)$$

$$v(t) = y(t) + w(t) \quad (9.48)$$

$$w(t) = v(t - T) \quad (9.49)$$

Applying the z-transform to the above three equations yields

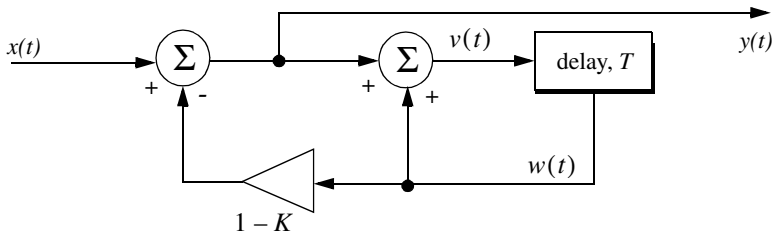


Figure 9.14. MTI recursive filter.

$$Y(z) = X(z) - (1 - K)W(z) \quad (9.50)$$

$$V(z) = Y(z) + W(z) \quad (9.51)$$

$$W(z) = z^{-1}V(z) \quad (9.52)$$

Solving for the transfer function $H(z) = Y(z)/X(z)$ yields

$$H(z) = \frac{1 - z^{-1}}{1 - Kz^{-1}} \quad (9.53)$$

The modulus square of $H(z)$ is then equal to

$$|H(z)|^2 = \frac{(1 - z^{-1})(1 - z)}{(1 - Kz^{-1})(1 - Kz)} = \frac{2 - (z + z^{-1})}{(1 + K^2) - K(z + z^{-1})} \quad (9.54)$$

Using the transformation $z = e^{j\omega T}$ yields

$$z + z^{-1} = 2 \cos \omega T \quad (9.55)$$

Thus, Eq. (54) can now be rewritten as

$$|H(e^{j\omega T})|^2 = \frac{2(1 - \cos \omega T)}{(1 + K^2) - 2K \cos(\omega T)} \quad (9.56)$$

Note that when $K = 0$, Eq. (9.56) collapses to Eq. (9.42) (single line canceler). Fig. 9.15 shows a plot of Eq. (9.56) for $K = 0.25, 0.7, 0.9$. Clearly, by changing the gain factor K one can control of the filter response.

In order to avoid oscillation due to the positive feedback, the value of K should be less than unity. The value $(1 - K)^{-1}$ is normally equal to the number of pulses received from the target. For example, $K = 0.9$ corresponds to ten pulses, while $K = 0.98$ corresponds to about fifty pulses.

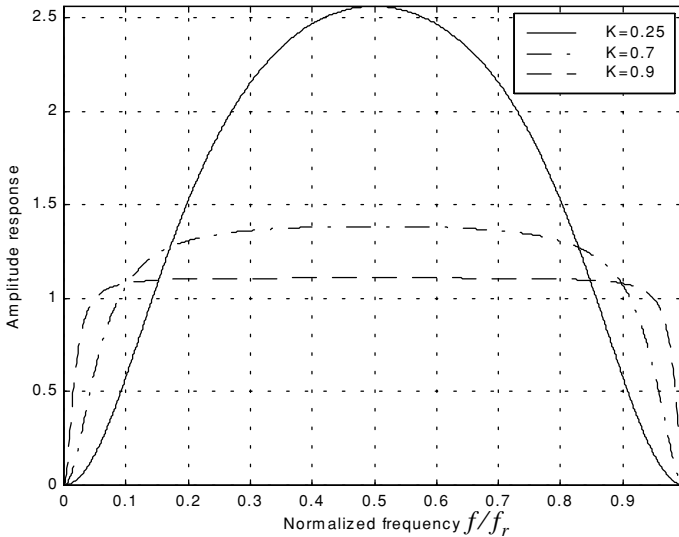


Figure 9.15. Frequency response corresponding to Eq. (9.56). This plot can be reproduced using MATLAB program “fig9_15.m” given in Listing 9.3 in Section 9.14.

9.10. PRF Staggering

Blind speeds can pose serious limitations on the performance of MTI radars and their ability to perform adequate target detection. Using PRF agility by changing the pulse repetition interval between consecutive pulses can extend

the first blind speed to tolerable values. In order to show how PRF staggering can alleviate the problem of blind speeds, let us first assume that two radars with distinct PRFs are utilized for detection. Since blind speeds are proportional to the PRF, the blind speeds of the two radars would be different. However, using two radars to alleviate the problem of blind speeds is a very costly option. A more practical solution is to use a single radar with two or more different PRFs.

For example, consider a radar system with two interpulse periods T_1 and T_2 , such that

$$\frac{T_1}{T_2} = \frac{n_1}{n_2} \quad (9.57)$$

where n_1 and n_2 are integers. The first true blind speed occurs when

$$\frac{n_1}{T_1} = \frac{n_2}{T_2} \quad (9.58)$$

This is illustrated in Fig. 9.16 for $n_1 = 4$ and $n_2 = 5$. Note that if $n_2 = n_1 + 1$, then the process of PRF staggering is similar to that discussed in Chapter 3.

The ratio

$$k_s = \frac{n_1}{n_2} \quad (9.59)$$

is known as the stagger ratio. Using staggering ratios closer to unity pushes the first true blind speed farther out. However, the dip in the vicinity of $1/T_1$ becomes deeper, as illustrated in Fig. 9.17 for stagger ratio $k_s = 63/64$. In general, if there are N PRFs related by

$$\frac{n_1}{T_1} = \frac{n_2}{T_2} = \dots = \frac{n_N}{T_N} \quad (9.60)$$

and if the first blind speed to occur for any of the individual PRFs is v_{blind1} , then the first true blind speed for the staggered waveform is

$$v_{blind} = \frac{n_1 + n_2 + \dots + n_N}{N} v_{blind1} \quad (9.61)$$

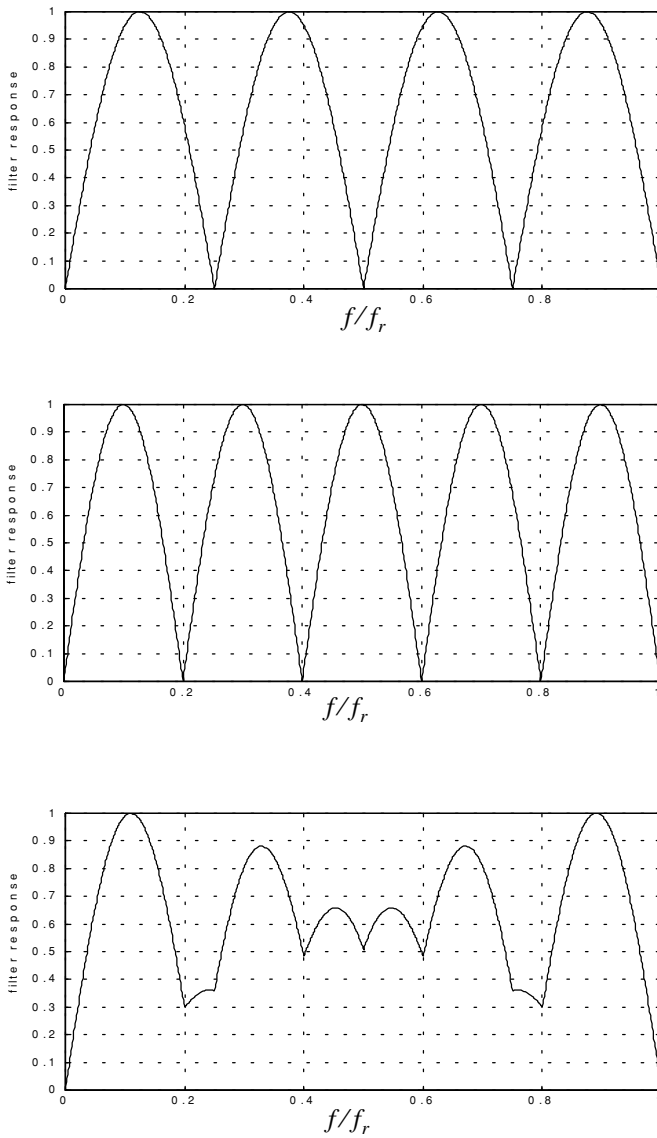


Figure 9.16. Frequency responses of a single canceler. Top plot corresponds to T_1 , middle plot corresponds to T_2 , bottom plot corresponds to stagger ratio $T_1/T_2 = 4/3$. This plot can be reproduced using MATLAB program “fig9_16.m” given in Listing 9.4 in Section 9.14.

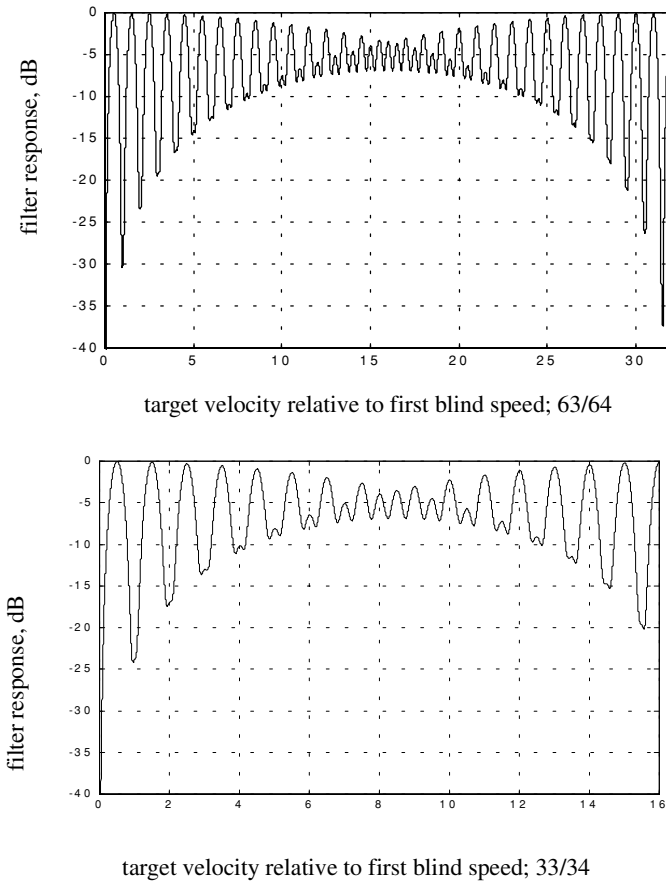


Figure 9.17. MTI responses, staggering ratio 63/64. This plot can be reproduced using MATLAB program “fig9_17.m” given in Listing 9.5 in Section 9.14.

9.11. MTI Improvement Factor

In this section two quantities that are normally used to define the performance of MTI systems are introduced. They are “Clutter Attenuation (CA)” and the MTI “Improvement Factor.” The MTI CA is defined as the ratio between the MTI filter input clutter power C_i to the output clutter power C_o ,

$$CA = C_i / C_o \quad (9.62)$$

The MTI improvement factor is defined as the ratio of the Signal to Clutter (SCR) at the output to the SCR at the input,

$$I = \left(\frac{S_o}{C_o}\right) / \left(\frac{S_i}{C_i}\right) \quad (9.63)$$

which can be rewritten as

$$I = \frac{S_o}{S_i} CA \quad (9.64)$$

The ratio S_o/S_i is the average power gain of the MTI filter, and it is equal to $|H(\omega)|^2$. In this section, a closed form expression for the improvement factor using a Gaussian-shaped power spectrum is developed. A Gaussian-shaped clutter power spectrum is given by

$$W(f) = \frac{P_c}{\sqrt{2\pi} \sigma_c} \exp(-f^2/2\sigma_c^2) \quad (9.65)$$

where P_c is the clutter power (constant), and σ_c is the clutter rms frequency and is given by

$$\sigma_c = 2\sigma_v/\lambda \quad (9.66)$$

where λ is the wavelength, and σ_v is the rms wind velocity, since wind is the main reason for clutter frequency spreading. Substituting Eq. (9.66) into Eq. (9.65) yields

$$W(f) = \frac{\lambda P_c}{2\sqrt{2\pi} \sigma_v} \exp\left(-\frac{f^2 \lambda^2}{8\sigma_v^2}\right) \quad (9.67)$$

The clutter power at the input of an MTI filter is

$$C_i = \int_{-\infty}^{\infty} \frac{P_c}{\sqrt{2\pi} \sigma_c} \exp\left(-\frac{f^2}{2\sigma_c^2}\right) df \quad (9.68)$$

Factoring out the constant P_c yields

$$C_i = P_c \int_{-\infty}^{\infty} \frac{1}{\sqrt{2\pi} \sigma_c} \exp\left(-\frac{f^2}{2\sigma_c^2}\right) df \quad (9.69)$$

It follows that (Why?)

$$C_i = P_c \quad (9.70)$$

The clutter power at the output of an MTI is

$$C_o = \int_{-\infty}^{\infty} W(f) |H(f)|^2 df \quad (9.71)$$

We will continue the analysis using a single delay line canceler. The frequency response for a single delay line canceler is given by Eq. (9.38). The single canceler power gain is given in Eq. (9.42), which will be repeated here, in terms of f rather than ω , as Eq. (9.72),

$$|H(f)|^2 = 4 \left(\sin \left(\frac{\pi f}{f_r} \right) \right)^2 \quad (9.72)$$

It follows that

$$C_o = \int_{-\infty}^{\infty} \frac{P_c}{\sqrt{2\pi} \sigma_c} \exp \left(- \frac{f^2}{2\sigma_c^2} \right) 4 \left(\sin \left(\frac{\pi f}{f_r} \right) \right)^2 df \quad (9.73)$$

Now, since clutter power will only be significant for small f , then the ratio f/f_r is very small (i.e., $\sigma_c \ll f_r$). Consequently, by using the small angle approximation Eq. (9.73) is approximated by

$$C_o \approx \int_{-\infty}^{\infty} \frac{P_c}{\sqrt{2\pi} \sigma_c} \exp \left(- \frac{f^2}{2\sigma_c^2} \right) 4 \left(\frac{\pi f}{f_r} \right)^2 df \quad (9.74)$$

which can be rewritten as

$$C_o = \frac{4P_c \pi^2}{f_r^2} \int_{-\infty}^{\infty} \frac{1}{\sqrt{2\pi} \sigma_c} \exp \left(- \frac{f^2}{2\sigma_c^2} \right) f^2 df \quad (9.75)$$

The integral part in Eq. (9.75) is the second moment of a zero mean Gaussian distribution with variance σ_c^2 . Replacing the integral in Eq. (9.75) by σ_c^2 yields

$$C_o = \frac{4P_c \pi^2}{f_r^2} \sigma_c^2 \quad (9.76)$$

Substituting Eqs. (9.76) and (9.70) into Eq. (9.62) produces

$$CA = \frac{C_i}{C_o} = \left(\frac{f_r}{2\pi\sigma_c} \right)^2 \quad (9.77)$$

It follows that the improvement factor for a single canceler is

$$I = \left(\frac{f_r}{2\pi\sigma_c} \right)^2 \frac{S_o}{S_i} \quad (9.78)$$

The power gain ratio for a single canceler is (remember that $|H(f)|$ is periodic with period f_r)

$$\frac{S_o}{S_i} = |H(f)|^2 = \frac{1}{f_r} \int_{-f_r/2}^{f_r/2} 4 \left(\sin \frac{\pi f}{f_r} \right)^2 df \quad (9.79)$$

Using the trigonometric identity $(2 - 2\cos 2\vartheta) = 4(\sin \vartheta)^2$ yields

$$|H(f)|^2 = \frac{1}{f_r} \int_{-f_r/2}^{f_r/2} \left(2 - 2\cos \frac{2\pi f}{f_r} \right) df = 2 \quad (9.80)$$

It follows that

$$I = 2(f_r / (2\pi\sigma_c))^2 \quad (9.81)$$

The expression given in Eq. (9.81) is an approximation valid only for $\sigma_c \ll f_r$. When the condition $\sigma_c \ll f_r$ is not true, then the autocorrelation function needs to be used in order to develop an exact expression for the improvement factor.

Example 9.3: A certain radar has $f_r = 800\text{Hz}$. If the clutter rms is $\sigma_c = 6.4\text{Hz}$ (wooded hills with $\sigma_v = 1.16311\text{Km/hr}$), find the improvement factor when a single delay line canceler is used.

Solution: The clutter attenuation CA is

$$CA = \left(\frac{f_r}{2\pi\sigma_c} \right)^2 = \left(\frac{800}{(2\pi)(6.4)} \right)^2 = 395.771 = 25.974\text{dB}$$

and since $S_o/S_i = 2 = 3\text{dB}$ we get

$$I_{dB} = (CA + S_o/S_i)_{dB} = 3 + 25.97 = 28.974\text{dB}.$$

9.12. Subclutter Visibility (SCV)

The phrase Subclutter Visibility (SCV) describes the radar's ability to detect non-stationary targets embedded in a strong clutter background, for some

probabilities of detection and false alarm. It is often used as a measure of MTI performance. For example, a radar with 10dB subclutter visibility will be able to detect moving targets whose returns are ten times smaller than those of clutter. A sketch illustrating the concept of SCV is shown in Fig. 9.18.

If a radar system can resolve the areas of strong and weak clutter within its field of view, then the phrase Interclutter Visibility (ICV) describes the radar's ability to detect non-stationary targets between strong clutter points. The subclutter visibility is expressed as the ratio of the improvement factor to the minimum MTI output SCR required for proper detection for a given probability of detection. More precisely,

$$SCV = I/(SCR)_o \tag{9.82}$$

When comparing different radar systems' performances on the basis of SCV, one should use caution since the amount of clutter power is dependent on the radar resolution cell (or volume), which may be different from one radar to another. Thus, only if the different radars have the same beam widths and the same pulse widths can SCV be used as a basis of performance comparison.

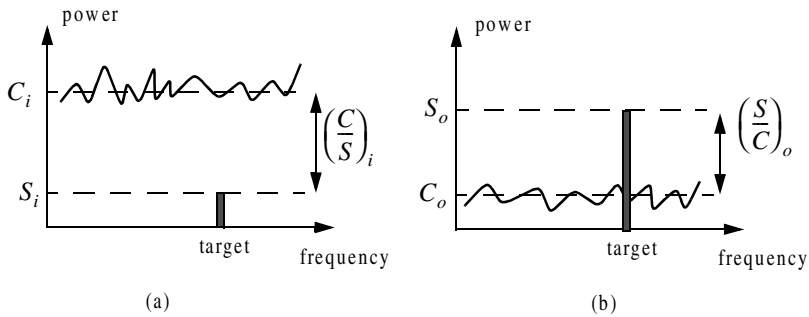


Figure 9.18. Illustration of SCV. (a) MTI input. (b) MTI output.

9.13. Delay Line Cancelers with Optimal Weights

The delay line cancelers discussed in this chapter belong to a family of transversal Finite Impulse Response (FIR) filters widely known as the "tapped delay line" filters. Fig. 9.19 shows an N-stage tapped delay line implementation.

When the weights are chosen such that they are the binomial coefficients (coefficients of the expansion $(1-x)^N$) with alternating signs, then the resultant MTI filter is equivalent to N-stage cascaded single line cancelers. This is illustrated in Fig. 9.20 for $N = 4$. In general, the binomial coefficients are given by

$$w_i = (-1)^{i-1} \frac{N!}{(N-i+1)!(i-1)!} ; i = 1, \dots, N+1 \quad (9.83)$$

Using the binomial coefficients with alternating signs produces an MTI filter that closely approximates the optimal filter in the sense that it maximizes the improvement factor, as well as the probability of detection. In fact, the difference between an optimal filter and one with binomial coefficients is so small that the latter one is considered to be optimal by most radar designers. However, being optimal in the sense of the improvement factor does not guarantee a deep notch, nor a flat pass-band in the MTI filter response. Consequently, many researchers have been investigating other weights that can produce a deeper notch around DC, as well as a better pass-band response.

In general, the average power gain for an N-stage delay line canceler is

$$\frac{S_o}{S_i} = \prod_{i=1}^N |H_1(f)|^2 = \prod_{i=1}^N 4 \left(\sin \left(\frac{\pi f}{f_r} \right) \right)^2 \quad (9.84)$$

where $|H_1(f)|^2$ is given in Eq. (9.72). For example, $N = 2$ (double delay line canceler) gives

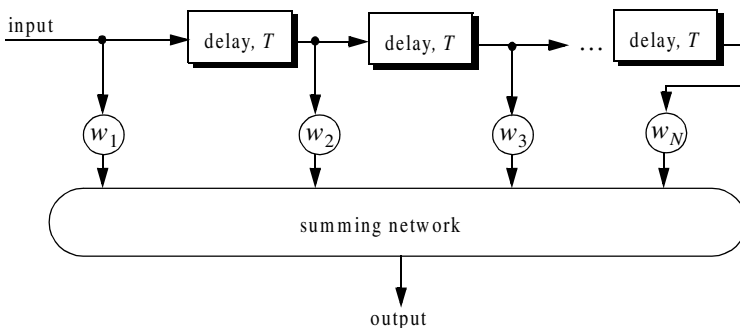


Figure 9.19. N-stage tapped delay line filter.

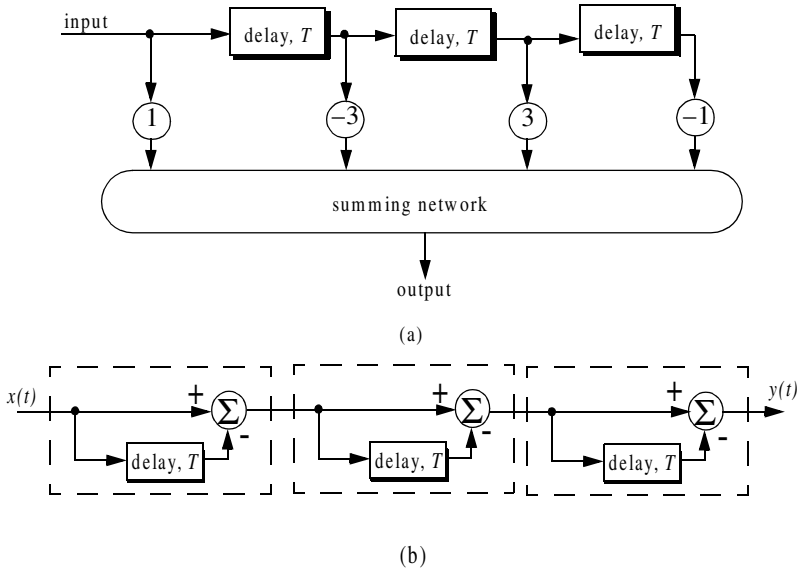


Figure 9.20. Two equivalent three delay line cancelers.
(a) Tapped delay line.
(b) Three cascaded single line cancelers.

$$\frac{S_o}{S_i} = 16 \left(\sin \left(\frac{\pi f}{f_r} \right) \right)^4 \tag{9.85}$$

Equation (9.84) can be rewritten as

$$\frac{S_o}{S_i} = |H_1(f)|^{2N} = 2^{2N} \left(\sin \left(\frac{\pi f}{f_r} \right) \right)^{2N} \tag{9.86}$$

As indicated by Eq. (9.86), blind speeds for an N-stage delay canceler are identical to those of a single canceler. It follows that blind speeds are independent from the number of cancelers used. It is possible to show that Eq. (9.86) can be written as

$$\frac{S_o}{S_i} = 1 + N^2 + \left(\frac{N(N-1)}{2!} \right)^2 + \left(\frac{N(N-1)(N-2)}{3!} \right)^2 + \dots \tag{9.87}$$

A general expression for the improvement factor of an N-stage tapped delay line canceler is reported by Nathanson¹ to be

1. Nathanson, F. E., *Radar Design Principles*, second edition, McGraw-Hill, Inc., 1991.

$$I = \frac{(S_o/S_i)}{N \sum_{k=1}^N \sum_{j=1}^N w_k w_j^* \rho\left(\frac{(k-j)}{f_r}\right)} \quad (9.88)$$

where the weights w_k and w_j are those of a tapped delay line canceler, and $\rho((k-j)/f_r)$ is the correlation coefficient between the k th and j th samples. For example, $N = 2$ produces

$$I = \frac{1}{1 - \frac{4}{3}\rho T + \frac{1}{3}\rho^2 T} \quad (9.89)$$

9.14. MATLAB Program/Function Listings

This section contains listings of all MATLAB programs and functions used in this chapter. Users are encouraged to rerun these codes with different inputs in order to enhance their understanding of the theory.

Listing 9.1. MATLAB Function “single_canceler.m”

```
function [resp] = single_canceler (fofr1)
eps = 0.00001;
fofr = 0:0.01:fofr1;
arg1 = pi .* fofr;
resp = 4.0 .* ((sin(arg1)).^2);
max1 = max(resp);
resp = resp ./ max1;
subplot(2,1,1)
plot(fofr,resp,'k')
xlabel ('Normalized frequency - f/fr')
ylabel ('Amplitude response - Volts')
grid
subplot(2,1,2)
resp=10.*log10(resp+eps);
plot(fofr,resp,'k');
axis tight
grid
xlabel ('Normalized frequency - f/fr')
ylabel ('Amplitude response - dB')
```

Listing 9.2. MATLAB Function “double_canceler.m”

```
function [resp] = double_canceler(fofr1)
eps = 0.00001;
fofr = 0:0.01:fofr1;
arg1 = pi .* fofr;
resp = 4.0 .* ((sin(arg1)).^2);
max1 = max(resp);
resp = resp ./ max1;
resp2 = resp .* resp;
subplot(2,1,1);
plot(fofr,resp,'k--',fofr, resp2,'k');
ylabel('Amplitude response - Volts')
resp2 = 20. .* log10(resp2+eps);
resp1 = 20. .* log10(resp+eps);
subplot(2,1,2)
plot(fofr,resp1,'k--',fofr,resp2,'k');
legend('single canceler','double canceler')
xlabel('Normalized frequency f/fofr')
ylabel('Amplitude response - Volts')
```

Listing 9.3. MATLAB Program “fig9_15.m”

```
clear all
fofr = 0:0.001:1;
arg = 2.*pi.*fofr;
nume = 2.*(1.-cos(arg));
den11 = (1. + 0.25 * 0.25);
den12 = (2. * 0.25) .* cos(arg);
den1 = den11 - den12;
den21 = 1.0 + 0.7 * 0.7;
den22 = (2. * 0.7) .* cos(arg);
den2 = den21 - den22;
den31 = (1.0 + 0.9 * 0.9);
den32 = ((2. * 0.9) .* cos(arg));
den3 = den31 - den32;
resp1 = nume ./ den1;
resp2 = nume ./ den2;
resp3 = nume ./ den3;
plot(fofr,resp1,'k',fofr,resp2,'k-',fofr,resp3,'k--');
xlabel('Normalized frequency')
ylabel('Amplitude response')
legend('K=0.25','K=0.7','K=0.9')
grid
axis tight
```

Listing 9.4. MATLAB Program “fig9_16.m”

```
clear all
fofr = 0:0.001:1;
f1 = 4.0 .* fofr;
f2 = 5.0 .* fofr;
arg1 = pi .* f1;
arg2 = pi .* f2;
resp1 = abs(sin(arg1));
resp2 = abs(sin(arg2));
resp = resp1+resp2;
max1 = max(resp);
resp = resp./max1;
plot(fofr,resp1,fofr,resp2,fofr,resp);
xlabel('Normalized frequency f/fr')
ylabel('Filter response')
```

Listing 9.5. MATLAB Program “fig9_17.m”

```
clear all
fofr = 0.01:0.001:32;
a = 63.0 / 64.0;
term1 = (1. - 2.0 .* cos(a*2*pi*fofr) + cos(4*pi*fofr)).^2;
term2 = (-2. .* sin(a*2*pi*fofr) + sin(4*pi*fofr)).^2;
resp = 0.25 .* sqrt(term1 + term2);
resp = 10. .* log(resp);
plot(fofr,resp);
axis([0 32 -40 0]);
grid
```

Problems

9.1. Compute the signal-to-clutter ratio (SCR) for the radar described in Example 9.1. In this case, assume antenna 3dB beam width $\theta_{3dB} = 0.03rad$, pulse width $\tau = 10\mu s$, range $R = 50Km$, grazing angle $\psi_g = 15^\circ$, target RCS $\sigma_t = 0.1m^2$, and clutter reflection coefficient $\sigma^0 = 0.02(m^2/m^2)$.

9.2. Repeat Example 9.2 for target RCS $\sigma_t = 0.15m^2$, pulse width $\tau = 0.1\mu s$, antenna beam width $\theta_a = \theta_e = 0.03radians$; the detection range is $R = 100Km$, and $\sum \sigma_i = 1.6 \times 10^{-9}(m^2/m^3)$.

9.3. The quadrature components of the clutter power spectrum are, respectively, given by

$$\bar{S}_I(f) = \delta(f) + \frac{C}{\sqrt{2\pi}\sigma_c} \exp(-f^2/2\sigma_c^2)$$

$$\bar{S}_Q(f) = \frac{C}{\sqrt{2\pi}\sigma_c} \exp(-f^2/2\sigma_c^2)$$

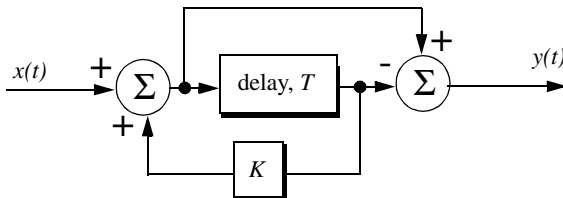
Compute the D.C. and A.C. power of the clutter. Let $\sigma_c = 10\text{Hz}$.

9.4. A certain radar has the following specifications: pulse width $\tau' = 1\mu\text{s}$, antenna beam width $\Omega = 1.5^\circ$, and wavelength $\lambda = 3\text{cm}$. The radar antenna is 7.5m high. A certain target is simulated by two point targets (scatterers). The first scatterer is 4m high and has RCS $\sigma_1 = 20\text{m}^2$. The second scatterer is 12m high and has RCS $\sigma_2 = 1\text{m}^2$. If the target is detected at 10Km , compute (a) SCR when both scatterers are observed by the radar; (b) the SCR when only the first scatterer is observed by the radar. Assume a reflection coefficient of -1 , and $\sigma^0 = -30\text{dB}$.

9.5. A certain radar has range resolution of 300m and is observing a target somewhere in a line of high towers each having RCS $\sigma_{tower} = 10^6\text{m}^2$. If the target has RCS $\sigma_t = 1\text{m}^2$, (a) How much signal-to-clutter ratio should the radar have? (b) Repeat part a for range resolution of 30m .

9.6. (a) Derive an expression for the impulse response of a single delay line canceler. (b) Repeat for a double delay line canceler.

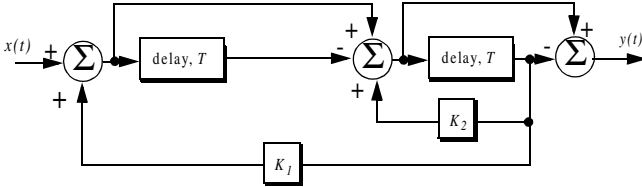
9.7. One implementation of a single delay line canceler with feedback is shown below:



(a) What is the transfer function, $H(z)$? (b) If the clutter power spectrum is $W(f) = w_0 \exp(-f^2/2\sigma_c^2)$, find an exact expression for the filter power gain. (c) Repeat part b for small values of frequency, f . (d) Compute the clutter attenuation and the improvement factor in terms of K and σ_c .

9.8. Plot the frequency response for the filter described in the previous problem for $K = -0.5, 0,$ and 0.5 .

9.9. An implementation of a double delay line canceler with feedback is shown below:



(a) What is the transfer function, $H(z)$? (b) Plot the frequency response for $K_1 = 0 = K_2$, and $K_1 = 0.2, K_2 = 0.5$.

9.10. Consider a single delay line canceler. Calculate the clutter attenuation and the improvement factor. Assume that $\sigma_c = 4Hz$ and a PRF $f_r = 450Hz$.

9.11. Develop an expression for the improvement factor of a double delay line canceler.

9.12. Repeat Problem 9.10 for a double delay line canceler.

9.13. An experimental expression for the clutter power spectrum density is $W(f) = w_0 \exp(-f^2/2\sigma_c^2)$, where w_0 is a constant. Show that using this expression leads to the same result obtained for the improvement factor as developed in Section 9.11.

9.14. Repeat Problem 9.13 for a double delay line canceler.

9.15. A certain radar uses two PRFs with stagger ratio 63/64. If the first PRF is $f_{r1} = 500Hz$, compute the blind speeds for both PRFs and for the resultant composite PRF. Assume $\lambda = 3cm$.

9.16. A certain filter used for clutter rejection has an impulse response $h(n) = \delta(n) - 3\delta(n-1) + 3\delta(n-2) - \delta(n-3)$. (a) Show an implementation of this filter using delay lines and adders. (b) What is the transfer function? (c) Plot the frequency response of this filter. (d) Calculate the output when the input is the unit step sequence.

9.17. The quadrature components of the clutter power spectrum are given in Problem 9.3. Let $\sigma_c = 10Hz$ and $f_r = 500Hz$. Compute the improvement of the signal-to-clutter ratio when a double delay line canceler is utilized.

9.18. Develop an expression for the clutter improvement factor for single and double line cancelers using the clutter autocorrelation function. Assume that the clutter power spectrum is as defined in Eq. (9.65).